

See discussions, stats, and author profiles for this publication at: <http://www.researchgate.net/publication/236152256>

# Boronic acid dendrimer receptor modified nanofibrillar cellulose membranes

ARTICLE in JOURNAL OF MATERIALS CHEMISTRY · JANUARY 2010

Impact Factor: 7.44 · DOI: 10.1039/b918308f

---

CITATIONS

18

---

READS

114

12 AUTHORS, INCLUDING:



**Tony D James**

University of Bath

239 PUBLICATIONS 7,038 CITATIONS

SEE PROFILE



**Karen Edler**

University of Bath

114 PUBLICATIONS 1,227 CITATIONS

SEE PROFILE



**Wim Thielemans**

University of Leuven

76 PUBLICATIONS 2,247 CITATIONS

SEE PROFILE



**Eleftheria Psillakis**

Technical University of Crete

84 PUBLICATIONS 3,251 CITATIONS

SEE PROFILE

# Boronic acid dendrimer receptor modified nanofibrillar cellulose membranes

Michael J. Bonn e,<sup>a</sup> Ewan Galbraith,<sup>a</sup> Tony D. James,<sup>a</sup> Matthew J. Wasbrough,<sup>a</sup> Karen J. Edler,<sup>a</sup> A. Toby A. Jenkins,<sup>a</sup> Matthew Helton,<sup>b</sup> Anthony McKee,<sup>b</sup> Wim Thielemans,<sup>c</sup> Eleftheria Psillakis<sup>d</sup> and Frank Marken<sup>\*a</sup>

Received 4th September 2009, Accepted 26th October 2009

First published as an Advance Article on the web 13th November 2009

DOI: 10.1039/b918308f

Cellulose nanofibrils from sisal of typically 4–5 nm diameter and *ca.* 250 ± 100 nm length are reconstituted into thin films of *ca.* 6 µm thickness (or thicker freestanding films). Pure cellulose and cellulose composite films are obtained in a solvent evaporation process. A boronic acid appended dendrimer is embedded as a receptor in the nanofibrillar cellulose membrane. The number of boronic acid binding sites is controlled by varying the dendrimer content. The electrochemical and spectrophotometric properties of the nanocomposite membrane are investigated using the probe molecule alizarin red S. Pure cellulose membranes inhibit access to the electrode. However, the presence of boronic acid receptor sites allows accumulation of alizarin red S with a Langmuirian binding constant of *ca.* 6000 ± 1000 M<sup>-1</sup>. The 2-electron 2-proton reduction of immobilized alizarin red S is shown to occur in a *ca.* 60 nm zone close to the electrode surface. With a boronic acid dendrimer modified nanofibrillar cellulose composition of 96 wt% cellulose and 4 wt% boronic acid dendrimer, the analytical range for alizarin red S in aqueous acetate buffer pH 3 is approximately 10 µM to 1 mM.

## 1. Introduction

Cellulose is an important natural raw material with a wide range of technical applications. Due to its inherent structural rigidity and high surface area<sup>1,2</sup> cellulose has been employed in liquid chromatography,<sup>3</sup> partially permeable membranes,<sup>4</sup> and in dialysis.<sup>5</sup> Cellulose can be derived from a variety of natural sources such as cotton,<sup>6</sup> bacteria,<sup>7</sup> straw,<sup>8</sup> and grass.<sup>9</sup> Extraction techniques such as acid hydrolysis<sup>10</sup> and enzymatic processes<sup>11</sup> allow cellulose raw materials to be converted into nanofibrillar cellulose. There are several different polymorphs of cellulose depending on its source and method of refinement. Most natural celluloses can be digested from their hierarchical structures into nanofibrils with a cellulose type-I crystal structure.<sup>12</sup> With ribbon shape and typical diameters of between 4 and 20 nm and with varying lengths often several hundred nanometres long,<sup>13</sup> these nanofibrils can be obtained and stabilized in the form of colloidal aqueous solutions.<sup>10</sup> The self-assembly or reconstitution of these cellulose nanofibrils has been of considerable recent interest with a view to mimicking or superceding current cellulose architectures for application in textiles, biocomposites, and sensors.<sup>14</sup>

The selective absorption and detection of analytes at modified electrode surfaces is an important area, for example, for the development of selective sensors with low limits of detection. Modified electrodes have been used to detect analytes including DNA,<sup>15</sup> dopamine,<sup>16</sup> histamine,<sup>17</sup> and glucose.<sup>18</sup> We have recently demonstrated the formation of cellulose composite structures at electrode surfaces using components such as TiO<sub>2</sub> nanoparticles<sup>19</sup> or cationic binding ionomers.<sup>20,21</sup> The inert and biocompatible nature of the cellulose matrix makes it an ideal material for sensing environmental and physiological analytes. The introduction of anionic surface groups on the cellulose nanoparticles results in a permselective film when deposited on an electrode.<sup>20b</sup> The incorporation of “receptor sites” within the cellulose matrix can add chemical selectivity. Here, the introduction of boronic acid binding sites into the cellulose matrix is investigated. The binding of boronic acid derivatives to various diol, carbohydrate, or amino acid analytes is well known<sup>22</sup> and there are examples of a stereospecific receptor-like binding.<sup>23</sup> Boronic acids have been suggested for *in vivo* sensing of D-glucose and similar physiological analytes.<sup>24</sup>

In this study, a boronic acid appended dendrimer (PAMAM generation 1) is employed embedded in cellulose nanofibrils. Boronic acid modified electrodes are useful tools in electroanalysis.<sup>25</sup> Recent research in the area of the electro-co-deposition of phenylboronic acid with poly-aniline has yielded a novel saccharide detector.<sup>26</sup> Here, we demonstrate that the combination of a boronic acid dendrimer with nanofibrillar cellulose by solvent evaporation with an aqueous casting solution produces stable membranes for spectrophotometric or electrochemical detection. The physical properties of the membranes are characterized and binding to alizarin red S is used to determine boronic acid site number and activity.

<sup>a</sup>Department of Chemistry, University of Bath, Claverton Down, UK Bath BA2 7AY. E-mail: F.Marken@bath.ac.uk

<sup>b</sup>Unilever Research & Development Port Sunlight, Quarry Road, East Bebington, Wirral, UK CH63 3JW

<sup>c</sup>School of Chemistry and Process and Environmental Research Division-Faculty of Engineering, University of Nottingham, University Park, Nottingham, UK NG7 2RD

<sup>d</sup>Laboratory of Aquatic Chemistry, Department of Environmental Engineering, Technical University of Crete, Polytechniopolis, 73100 Chania-Crete, Greece

## 2. Experimental methods

### 2.1. Chemical reagents

Acetic acid, sodium acetate trihydrate, and alizarin red S were obtained from Aldrich and used without further purification. Cellulose nanofibrils 0.69 wt% solutions in water were prepared from sisal following a literature procedure.<sup>10</sup> Demineralized and filtered water was taken from a Vivendi water purification system (Vivendi, High Wycombe, Bucks) with a resistivity of not less than 18 Mohm cm.

### 2.2. Instrumentation

For voltammetric studies a microAutolab II potentiostat system (EcoChemie, NL) was employed with a Pt gauze counter electrode and a saturated Calomel (SCE) reference electrode (REF401, Radiometer, Copenhagen). The working electrode was a 3 mm diameter glassy carbon electrode (BAS, US). Experiments were conducted after de-aerating with high purity argon (BOC) for at least 15 min prior to recording voltammograms. The temperature during experiments was  $20 \pm 2$  °C.

UV-visible spectra were obtained using a VISION Lite UV-vis spectrometer over a wavelength range of 350–800 nm. For surface topography imaging an atomic force microscope (Digital Instruments Nanoscope III, used in contact mode) was employed. A SAXS–WAXS (simultaneous small-angle X-ray scattering and wide-angle X-ray scattering) pattern of cellulose membranes was obtained on an Anton Paar SAXSess system using a PANalytical PW3830 X-ray generator. The X-ray image plates were observed using a Perkin Elmer Cyclone Storage Phosphor System. The small-angle patterns were recorded with Cu K $\alpha$  radiation ( $\lambda = 1.5406$  Å) at 40 kV and 50 mA in the region of  $2\theta$  from 5° to 25° with an exposure time of 45 min whilst simultaneous recording small-angle patterns in the region of 0.2 Å to 100 Å.

### 2.3. Synthesis of boronic acid dendrimer

Synthesis of boronic acid appended dendrimer: 200 mg, 0.14 mmol (as 1.0 g of a 20 wt% solution in MeOH) of generation 1 PAMAM dendrimer (ethylenediamine core, 8 amino surface groups), were diluted in a further 10 mL dry methanol and stirred at 60 °C in the presence of a 16-fold excess of 2-formylphenylboronic acid (2.24 mmol, 360 mg) for 48 h under nitrogen gas atmosphere. The solution was then cooled to 0 °C (ice/water bath) and NaBH<sub>4</sub> (169 mg, 4.48 mmol) was added portion-wise under a stream of nitrogen to the stirring mixture. The suspension was allowed to warm to room temperature and stirred for a further 8 h. 2 M HCl (aq) was slowly added until no further gas was evolved and the solution was stirred for 2 h. The resulting crude material was neutralized with NaOH (aq) and diluted further with water (5 mL) and methanol (5 mL) and then passed through an ultrafiltration membrane (MWCO 1000) at 62 psi nitrogen pressure in a Millipore stirred cell. Further concentration with  $2 \times 5$  mL 10% methanol (aq) was performed using the same apparatus. The remaining residue was retrieved by dissolving in methanol and subsequently dried by evaporation at reduced pressure. Isolated yield of colourless gum was 287 mg (82%).

$\delta_{\text{H}}$  (300 MHz, d<sub>4</sub>-MeOD) 7.33–7.31 (8H, m), 7.12–7.09 (16H, m), 7.07–7.03 (8H, m), 3.96 (16H, s), 3.43 (16H, t,  $J = 6$  Hz), 2.89

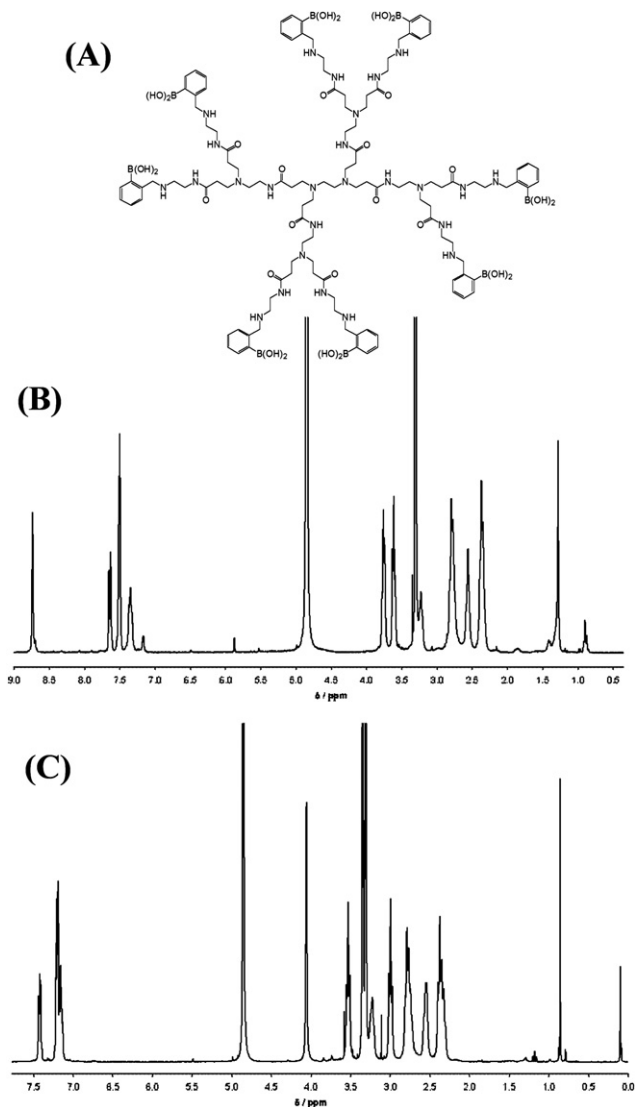


**Fig. 1** (A) Chemical structure of the boronic acid dendrimer 1. (B) The <sup>1</sup>H NMR spectrum (300 MHz, d<sub>4</sub>-MeOD) for the isolated imine intermediate. (C) The <sup>1</sup>H NMR spectrum (300 MHz, d<sub>4</sub>-MeOD) for pure dendrimer 1.

(16H, t,  $J = 6$  Hz), 2.71–2.62 (24H, m), 2.46–2.44 (16H, m), 2.30–2.21 (28H, m);  $\delta_{\text{C}}$  (75.5 MHz, d<sub>4</sub>-MeOD) 178.5, 177.68, 145.6, 134.4, 131.4, 130.7, 127.0, 58.0, 56.4, 54.0, 41.5, 41.0, 37.7;  $\delta_{\text{B}}$  NMR (96.3 MHz, d-MeOD) 10.3. It is worth noting that boronic acids are notoriously difficult to characterize. No suitable elemental analysis can be obtained for dendrimer 1. This is a well documented problem encountered with many boronic acid compounds, where incomplete sample combustion gives erroneous results.<sup>27</sup> Mass spectral analysis is also difficult due to dehydration and crosslinking of the boronic acid groups. Proton NMR data are provided here in Fig. 1C to prove dendrimer purity.

### 2.4. Formation of boronic acid dendrimer modified nanofibrillar cellulose membranes

Nanocomposite membranes of boronic acid dendrimer and cellulose nanofibrils were formed using a solvent casting

technique. Boronic acid appended dendrimer was dissolved in 10 mL of methanol to give a 13.9 mg mL<sup>-1</sup> solution. This solution (in appropriate amounts) was directly added to 1 mL aqueous cellulose solution (0.69 wt% nanofibrils) and thoroughly mixed. For example, 20  $\mu$ L of the boronic acid dendrimer–methanol solution were added to 1 mL of cellulose solution and then vigorously agitated (by ultrasonication). A 5  $\mu$ L volume of this solution was placed on the surface of a clean glassy carbon electrode and then dried in an oven at 60 °C for 1 h. This resulted in a film with 4 wt% boronic acid dendrimer to 96 wt% cellulose nanofibrils. Freestanding membranes were required for SAXS–WAXS experiments. These membranes were prepared by placing 1 mL of deposition solution onto a flat Teflon substrate (area *ca.* 2 cm<sup>2</sup>), drying in an oven at 60 °C for 1 h, and peeling off the resulting membrane from the Teflon surface with a pair of tweezers. The membranes were then left to equilibrate at ambient temperature and humidity before conducting experiments.

### 2.5. Immobilization of alizarin red S in boronic acid modified nanofibrillar cellulose membranes

In order to bind alizarin red S into the modified cellulose films samples were immersed into aqueous solutions of alizarin red S in 0.1 M acetate buffer (pH adjusted from 3 to 7) for 30 min followed by thorough rinsing with deionized water for 10 s and drying in ambient conditions.

## 3. Results and discussion

### 3.1. Formation and characterization of boronic acid dendrimer modified nanofibrillar cellulose membranes

Membranes of nanofibrillar cellulose are readily obtained by evaporation of a nanocellulose sol in water on suitable substrates.<sup>20</sup> The cellulose nanofibrils are believed to crosslink *via* hydrogen bridges thereby forming strong and durable network membranes.<sup>20b</sup> It is possible to imbed reactive ionomer<sup>21</sup> molecules into these “reconstituted” cellulose membranes. In this study, a dendrimer system with the ability to act as a receptor for carbohydrates and catechols is used to functionalize cellulose films. The functionalization procedure is simple. In contrast to smaller molecular receptor systems with the ability to diffuse within the cellulose matrix, the dendrimer becomes immobilized into the cellulose nanofibril network.

Boronic acids are known to bind to polyols and carbohydrates<sup>28</sup> and they have been employed to provide functional surfaces in chromatography<sup>29</sup> *e.g.* for the separation of RNA.<sup>30</sup> Here, boronic acid appended dendrimers (generation 1 PAMAM) are employed to modify cellulose membranes. These modified cellulose membranes were formed in a solution evaporation process (see Experimental) based on an aqueous sol.

The topography and thickness of membranes were examined by atomic force microscopy (AFM) in tapping mode (see Fig. 2). Membranes were deposited onto quartz glass substrates from a 5  $\mu$ L volume of aqueous solution of cellulose nanofibrils (0.69 wt%) and boronic acid dendrimer (0.03 wt%) followed by drying for 60 min in an oven at 60 °C (giving a film containing 96% cellulose and 4% boronic acid dendrimer, see Experimental). Scratches were introduced using a scalpel in order to measure the thickness of membranes (not shown). The profile of the scratch

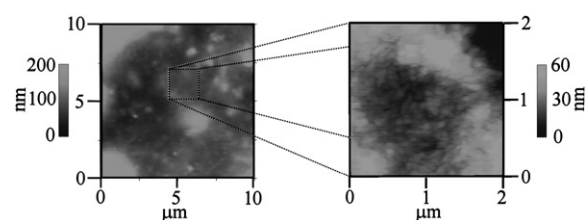


**Fig. 2** AFM images for a 96 wt% cellulose nanofibril–4 wt% boronic acid dendrimer membrane on a quartz glass substrate showing the topography of individual nanofibrils packed into a dense layer.

was compared at different locations on the membrane surface yielding an average thickness of approximately 3  $\mu$ m (for a *ca.* 5 mm diameter disc-shaped deposit) which suggests a typical membrane volume of  $6 \times 10^{-11}$  m<sup>3</sup> in 5  $\mu$ L deposition solution (the calculated membrane density is 0.6 g cm<sup>-3</sup> compared to the crystal density<sup>31</sup> of cellulose 1.582 g cm<sup>-3</sup>). The membrane topography (see Fig. 2) reveals poorly resolved cellulose nanofibrils with approximately  $250 \pm 100$  nm length. A 4–5 nm diameter for these nanofibrils has been reported based on values from TEM analysis.<sup>10</sup>

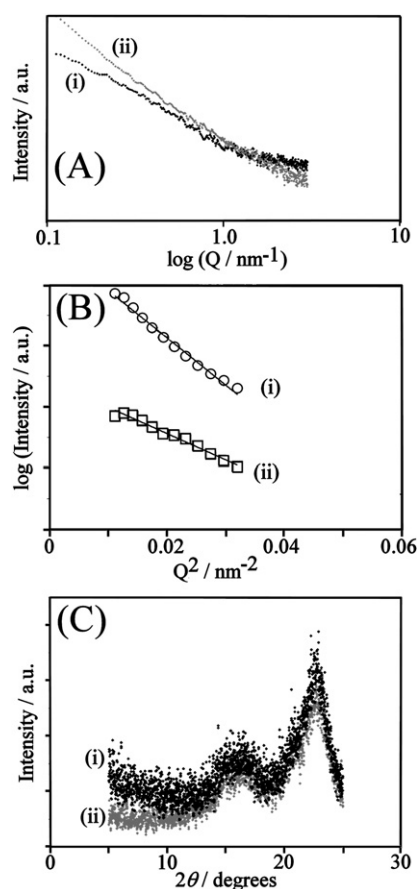


**Fig. 3** X-Ray scattering data for (i) nanofibrillar cellulose and (ii) for boronic acid dendrimer modified nanofibrillar cellulose (reconstituted 96 wt% cellulose nanofibrils and 4 wt% boronic acid dendrimer). (A) Small-angle scattering data. (B) A Guinier plot of the logarithm of intensity *versus* the momentum transfer squared,  $Q^2$ , giving approximate radii of gyration of (i)  $R_G = 11.4$  nm and (ii)  $R_G = 15.3$  nm. (C) Wide-angle X-ray scattering data.

X-Ray scattering techniques offer a powerful probe into both atomic and nanostructure of composite materials. Previous studies of cellulose nanofibril materials have shown that the nanofibrils have a ribbon morphology.<sup>32</sup> Here, the morphologies of both plain reconstituted cellulose nanofibrils and nanocellulose–boronic acid dendrimer composite membranes are investigated with wide and small-angle X-ray scattering techniques.

In Fig. 3A the small-angle X-ray scattering patterns are shown for (i) a nanocellulose membrane and (ii) a nanocellulose–boronic acid dendrimer modified membrane (96 wt% cellulose and 4 wt% boronic acid dendrimer). An approximately linear relationship between the scattering intensity,  $I$ , and the value of the momentum transfer,  $Q$  (which is given by  $Q = 4\pi/\lambda \sin(\theta)$  where  $\theta$  is half the scattering angle), is observed. Upon the introduction of boronic acid dendrimer into the cellulose membrane, there is a marked change in the slope of the SAXS pattern. Guinier analysis was applied to the experimental curves for both membranes. The expression  $\ln(I) = \ln(I_0) - (R_G^2/3) \times Q^2$  allows the radius of gyration,  $R_G$ , to be estimated as  $R_g(i) = 11.4$  nm and  $R_g(ii) = 15.3$  nm. The boronic acid dendrimer is clearly opening up the structure, and consistent with the approximate diameter of the spherical boronic acid dendrimer of *ca.* 4 nm whereby the presence of one dendrimer unit binding the cellulose nanofibrils together is confirmed. This result suggests an attractive interaction between boronic acid dendrimer and cellulose nanofibrils, although the nature of this interaction is currently unclear.

In the wide-angle X-ray scattering pattern (see Fig. 3C), characteristic cellulose type I crystal structure peaks are observed.<sup>33</sup> The data are consistent with scattering by the cellulose-I polymorph,<sup>34</sup> where the peaks occur at  $14.8^\circ$  (scattering from the 110 diffraction plane), at  $16.4^\circ$  (110 diffraction plane), and at  $22.6^\circ$  (020 diffraction plane). The additional peak found in the pattern at  $20.6^\circ$  (shoulder) could be due to small amount of polymorph or native cellulose-I $\alpha$ .<sup>35</sup>

### 3.2. Spectrophotometric and voltammetric study of alizarin red S binding into boronic acid dendrimer modified nanofibrillar cellulose membranes

Alizarin red S (3,4-dihydroxy-9,10-dioxo-2-anthracenesulfonic acid, sodium salt) is a common fluorescence probe<sup>36</sup> and analytical dye molecule.<sup>37</sup> It is used here to quantify binding to free boronic acids<sup>38</sup> within the cellulose membrane. Alizarin red S is a probe molecule with both spectrophotometric and electrochemical activity (in aqueous media a 2-electron 2-proton reversible reduction occurs<sup>39</sup>).

The UV-visible spectrum of alizarin red S was measured to determine the effect of binding into the boronic acid dendrimer modified nanofibrillar cellulose membranes. First, the solution phase absorbance was measured using solutions of 50  $\mu$ M alizarin red S in 0.1 M acetate buffer at pH 3 and at pH 7 (Fig. 4A). The  $pK_a$  of alizarin red S<sup>40</sup> for the first deprotonation step is  $\sim 4$  (see eqn (1)) and this leads to a characteristic change in colour from yellow to red. Therefore acetate buffer between pH 3 and pH 7 was employed to study this system. An absorbance peak at a wavelength of *ca.* 420 nm can be seen for the solution phase species at pH 3 with the maximum absorption wavelength

shifting to *ca.* 520 nm for alizarin red S at pH 7, consistent with literature reports.<sup>41</sup>

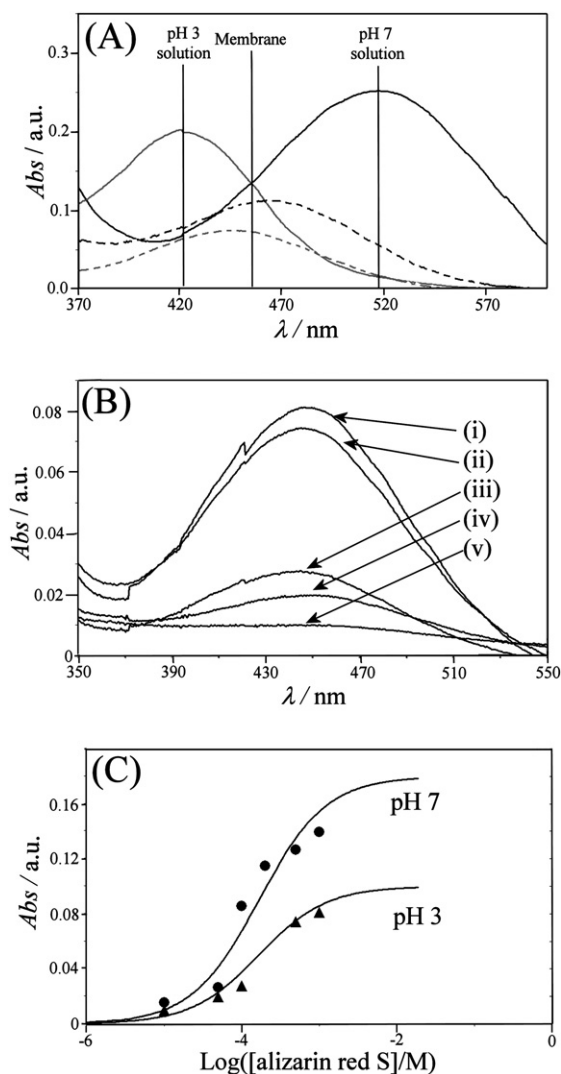
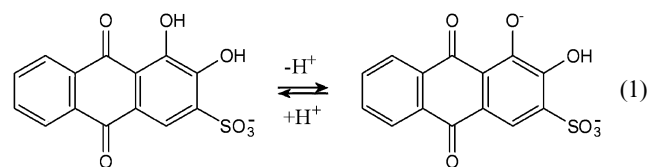
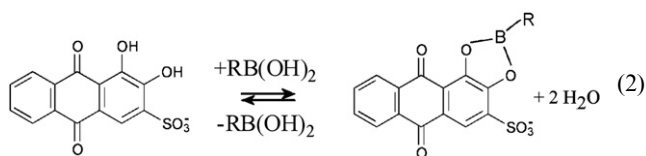


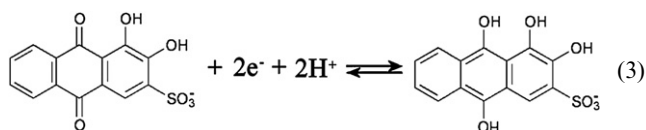
**Fig. 4** (A) UV-visible spectra of 50  $\mu$ M alizarin red S in 0.1 M acetate buffer at pH 3 (grey line,  $\lambda_{\max} \approx 420$  nm) and at pH 7 (black line,  $\lambda_{\max} \approx 520$  nm). Also shown are spectra for a boronic acid dendrimer modified nanofibrillar cellulose membrane soaked in 500  $\mu$ M alizarin red S with 0.1 M acetate buffer at pH 3 (grey dashed line) and at pH 7 (black dashed line) both with  $\lambda_{\max}$  *ca.* 455 nm. (B) UV-visible spectra for a boronic acid dendrimer modified nanofibrillar cellulose films soaked (i) 1000, (ii) 100, (iii) 50 and (v) 10  $\mu$ M alizarin red S in 0.1 M acetate buffer pH 3. (C) Langmuir plot of the UV-visible absorption for membrane samples *versus* the concentration of alizarin red S in the 0.1 M acetate buffer soaking solution for pH 3 and for pH 7. The lines show the expected behaviour for a Langmuirian binding constant  $K_{\text{obs}} = 6000 \text{ mol}^{-1} \text{ dm}^3$ .

Next, alizarin red S was bound into the boronic acid dendrimer modified nanofibrillar cellulose membrane. Films without and with boronic acid were formed by drying 0.5 mL of precursor solution on a 1 cm<sup>2</sup> transparent quartz glass substrate. The resulting membrane (thickness *ca.* 60 μm) was then immersed for 30 min in a solution of 500 μM alizarin red S in acetate buffer at pH 3 (or at pH 7). After rinsing and drying the transmission spectrum was recorded (see Fig. 4A). In the absence of the boronic acid dendrimer no strong binding of alizarin red S occurred. In the presence of the boronic acid dendrimer, a new absorption peak at ~455 nm is observed (see Fig. 4A) for both samples prepared at pH 3 and at pH 7. These characteristic absorption peaks are consistent with alizarin red S when bound to phenylboronic acids.<sup>42</sup> The minor shift in the wavelength of absorbance peaks for samples obtained at pH 3 and at pH 7 may be due to local changes in the chemical environment of the bound alizarin red S (see Fig. 4A). The difference in boronic acid bound and free alizarin red S clearly confirms binding *via* the boronic acid.

The binding of alizarin red S into the boronic acid dendrimer modified nanofibrillar cellulose membrane was investigated as a function of alizarin concentration (at pH 3 and at pH 7, see Fig. 4B and C). Analysis based on Langmuirian binding suggested a binding constant for alizarin red S of  $K_{\text{obs}} = 6000 \pm 1000 \text{ M}^{-1}$  very much consistent with literature reports on solution phase binding to boronic acids.<sup>43</sup> Similar results are obtained for binding at pH 3 and at pH 7. The binding of alizarin red S to a boronic acid occurs *via* the catechol moiety<sup>42</sup> (see eqn (2)). Note that the methylamine functionality *ortho* to the boronic acid (see structure in Fig. 1) further stabilizes the bound state by protecting the boron from nucleophile attack.



Next, voltammetry was used to detect and monitor the diffusion and binding of alizarin red S in the boronic acid dendrimer modified nanofibrillar cellulose membranes. At a bare glassy carbon electrode immersed in 1 mM alizarin red S in aqueous 0.1 M acetate buffer pH 3 an apparently well-defined chemically reversible voltammetric response is observed with a midpoint potential of *ca.* -0.37 V *vs.* SCE (see Fig. 5A). The reduction of alizarin red S follows a 2-electron 2-proton mechanism<sup>44</sup> (see eqn (3)).



Analysis of a plot of the logarithm of peak current *versus* the logarithm of scan rate (not shown) suggests a square root dependence on scan rate which suggests diffusion characteristics typical for processes in aqueous solution. Next, a film of boronic acid dendrimer modified nanofibrillar cellulose was applied to

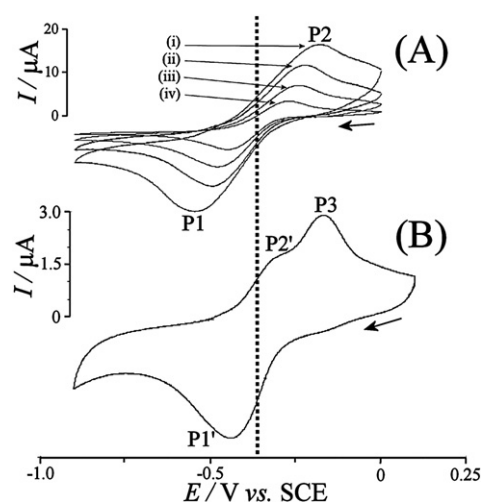
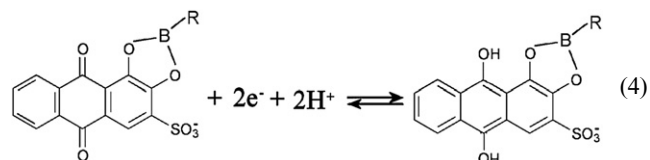


**Fig. 5** (A) Cyclic voltammograms (2<sup>nd</sup> scan shown) for the reduction and oxidation of 1 mM alizarin red S in 0.1 M acetate buffer pH 3 at a 3 mm diameter glassy carbon electrode 3 at scan rates of (i) 500, (ii) 200, (iii) 100 and (iv) 50 mV s<sup>-1</sup>. (B) Cyclic voltammograms (2<sup>nd</sup> scan shown, 100 mV s<sup>-1</sup>) for the oxidation and reduction of alizarin red S in a boronic acid dendrimer modified cellulose nanofibril membrane at a glassy carbon surface (immobilized by soaking in a 1 mM alizarin red S in 0.1 M acetate buffer pH 3 for 30 min) reimmersed in clean 0.1 M acetate buffer pH 3.

the glassy carbon electrode (thickness *ca.* 6 μm, *ca.* 96 wt% cellulose and 4 wt% boronic acid dendrimer) and modified by immersion into 1 mM alizarin red S in 0.1 M acetate buffer (pH 3) for a period of 30 min. The electrode was rinsed with deionized water and left to dry in ambient conditions before use in voltammetric experiments.

Fig. 5B shows typical voltammetric responses for the alizarin red S modified electrode immersed in 0.1 M acetate buffer pH 3. A cathodic peak at -0.47 V *vs.* SCE (P1') is observed followed by two anodic peaks (P2' and P3) at -0.32 and -0.17 V *vs.* SCE. When recorded at different scan rates, the peak current (P1') shows an approximately linear dependence on the scan rate consistent with an immobilized redox system. The reduction and re-oxidation process can be assigned to a 2-electron 2-proton process (see eqn (4)) similar to that observed for alizarin red S in solution. However, the process is confined to a small reaction zone close to the electrode surface.



The appearance of two oxidation peaks (see Fig. 5B) suggests that the reduction of the boronic acid bound alizarin red S is causing two distinct forms of alizarin red S to form. Experiments conducted over a range of scan rates (see Fig. 6A) confirm that the ratio of the peak currents for both peaks, P2' and P3, remains approximately constant. The peak response P2' is very similar to the corresponding reduction peak for the free alizarin red S

(P2 in Fig. 5A) and therefore a disproportionation mechanism is proposed. The formation of the reduced form of the boronic acid bound alizarin red S (see eqn (4)) causes two new phenolic binding sites for boronic acids to form. Rapid re-equilibration will cause more strongly bound alizarin red S to form with 3 or 4 phenolic O–B bonds whereas some alizarin red S molecules will be “freed” from the boronic acid binding. The oxidation of the “free” alizarin red S is assigned to process P2' whereas the oxidation of the more strongly bound alizarin red S is assigned to process P3. Alternatively, structural effects such as a change from 1,2-diol binding to 1,3-diol binding could also contribute to the observed peak splitting.

The effect of the number of boronic acid binding sites incorporated into the nanofibrillar cellulose membrane may be altered by changing the content of boronic acid dendrimer in the casting solution. In Fig. 6B, as the amount of boronic acid dendrimer present in the membrane is increased, the current response of the membrane with immobilized alizarin red S also increased. In order to quantify this effect, the charge under the cathodic current response (P2') was plotted *versus* the weight percentage of boronic acid dendrimer within the membranes (see Fig. 6D). With no boronic acid dendrimer present, there is

a residual voltammetric response due to alizarin red S physically retained in the membrane. Upon the introduction of boronic acid dendrimer the charge under the peak increases steadily until the boronic acid dendrimer content reaches *ca.* 8 wt%. In this composition range the voltammetric response is dominated by the boronic acid bound alizarin red S. For a membrane with 4 wt% boronic acid dendrimer content, a charge of  $\sim 7 \mu\text{C}$  was measured which equates to an amount of alizarin red S of *ca.* 40 pmol detectable in the membrane. This compares to an expected charge of 1 mC calculated based on the available boronic acid binding sites in the 6  $\mu\text{m}$  thick film (for a *ca.* 3.5 mm diameter disc-shaped deposit). Therefore only about 1% of the cellulose film (*ca.* 60 nm very close to the electrode surface) is electrochemically active. The likely reason for this low level of activity is a poor charge carrier mobility (neighboring alizarin red S molecules are not able to pass on the charge).

For a boronic acid dendrimer content of higher than  $\sim 8$  wt% the nanocomposite film becomes mechanically unstable and deterioration during voltammetric experiments is observed. Therefore, for all further voltammetric experiments a 4 wt% boronic acid dendrimer content was employed. The binding constant for the alizarin red S by the membrane,  $K_{\text{obs}}$ , was

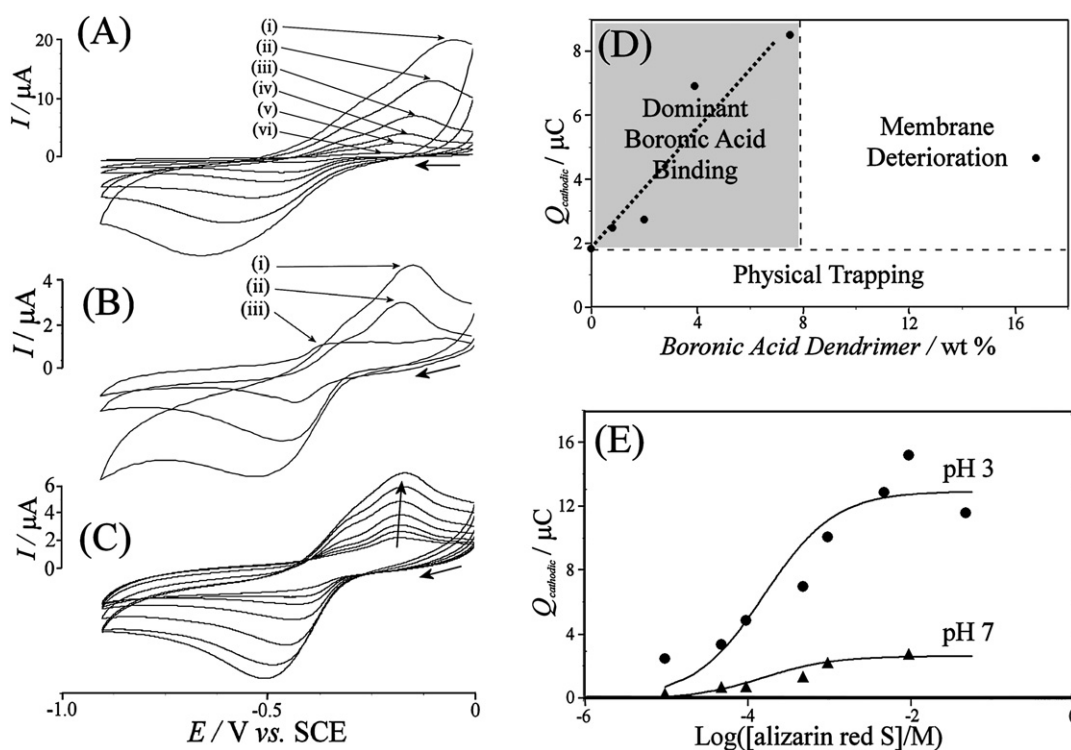


**Fig. 6** (A) Cyclic voltammograms (scan rate (i) 1000, (ii) 500, (iii) 200, (iv) 100, (v) 50, and (vi) 20  $\text{mV s}^{-1}$ , 2<sup>nd</sup> scan shown) for the reduction and re-oxidation of alizarin red S (immobilized by immersion into 1 mM alizarin red S in 0.1 M acetate buffer pH 3 for 30 min) at a boronic acid dendrimer modified cellulose film electrode (96 wt% cellulose and 4 wt% boronic acid dendrimer) immersed in 0.1 M acetate buffer pH 3. (B) Cyclic voltammograms (scan rate 100  $\text{mV s}^{-1}$ , 2<sup>nd</sup> scan shown) for the reduction and re-oxidation alizarin red S (immobilized by immersion into 1 mM alizarin red S in 0.1 M acetate buffer pH 3 for 30 min) at boronic acid dendrimer modified cellulose film electrodes with (i) 8 wt%, (ii) 4 wt% and (iii) 0 wt% boronic acid dendrimer. (C) Cyclic voltammograms (scan rate 100  $\text{mV s}^{-1}$ , 2<sup>nd</sup> scan shown) for the reduction and re-oxidation of alizarin red S (immobilized by immersion into alizarin red S with a concentration of  $10^{-5}$  to  $5 \times 10^{-2}$  M in 0.1 M acetate buffer pH 3 for 30 min) at a boronic acid dendrimer modified cellulose film electrode (96 wt% cellulose and 4 wt% boronic acid dendrimer) immersed in 0.1 M acetate buffer pH 3. (D) Plot of the charge under the reduction of alizarin red S when immobilized into boronic acid dendrimer modified cellulose *versus* boronic acid dendrimer content. (E) Langmuir isotherm plot for the charge under the alizarin red S reduction peak *versus* the concentration of alizarin red S during immobilization at pH 3 and at pH 7. The lines indicate the expected behaviour for a binding constant  $K = 6000 \pm 1000 \text{ mol}^{-1} \text{ dm}^3$ .

determined in acetate buffer at pH 3 and at pH 7. The concentration of alizarin red S was varied between 10  $\mu\text{M}$  and up to 50 mM (reaching the solubility limit). The charge under the reduction peak was plotted *versus* the alizarin red S concentration used during immobilization (see Fig. 6E). Assuming Langmuirian binding characteristics, the binding constant for alizarin red S in the membrane was obtained as  $K_{\text{obs}} = 6000 \pm 1000 \text{ M}^{-1}$  consistent with spectrophotometric measurements (*vide supra*). The effect of the pH on the binding constant appears to be insignificant. The difference in the magnitude of the charge under the reduction peak at pH 3 and at pH 7 can be explained for example with different charge carrier mobility for immobilized alizarin red S (see eqn (1)).

#### 4. Conclusions

Boronic acid dendrimer modified nanofibrillar cellulose membranes are stable for less than 8 wt% boronic acid dendrimer content. Boronic acid binding sites introduced into the film remain immobile due to the dendrimer structure and they allow alizarin red S absorption which was followed by both spectrophotometry and voltammetry. A Langmuir-type binding isotherm was observed with  $K = 6000 \pm 1000 \text{ M}^{-1}$  and with a linear alizarin red S detection range of *ca.* 10  $\mu\text{M}$  to 1 mM.

#### Acknowledgements

M.J.B. thanks Unilever Research & Development Port Sunlight for a PhD stipend and support. F.M. and E.P. thank the British Council for the award of a scientific exchange project entitled "Novel Environmental Technologies". W.T. thanks EPSRC for funding under the Driving Innovation in Chemistry and Chemical Engineering (DICE) Science and Innovation Award (Grant number EP/D501229/1).

#### References

- 1 T. Zimmermann, E. Pohler, T. Geiger, A. Schleuniger, P. Schwaller and M. Richter, *Cellulose Nanocomposites: Processing, Characterization, and Properties*, ACS Series 938, American Chemical Society, Washington, 2006, pp. 33–47.
- 2 Y. C. Hsieh, H. Yano, M. Nogi and S. J. Eichhorn, *Cellulose*, 2008, **15**, 507.
- 3 A. Potthast, T. Rosenau and P. Kosma, in *Polysaccharides II*, ed. D. Klemm, Springer, Berlin, Heidelberg, 2006, vol. 205, p. 1.
- 4 M. Cohen-Atiya, P. Vadgama and D. Mandler, *Soft Matter*, 2007, **3**, 1053.
- 5 M. Abe, F. Kikuchi, K. Kaizu and K. Matsumoto, *Clin. Nephrol.*, 2008, **69**, 354.
- 6 Y. Sun, L. Lin, C. S. Pang, H. B. Deng, H. Peng, J. Z. Li, B. H. He and S. Liu, *Energy Fuels*, 2007, **21**, 2386.
- 7 R. E. Cannon and S. M. Anderson, *Crit. Rev. Microbiol.*, 1991, **17**, 435.
- 8 N. Reddy and Y. Q. Yang, *J. Agric. Food Chem.*, 2007, **55**, 8570.
- 9 H. Hakansson, U. Germgard and D. Sens, *Cellulose*, 2005, **12**, 621.

- 10 N. L. Garcia de Rodriguez, W. Thielemans and A. Dufresne, *Cellulose*, 2006, **13**, 261.
- 11 A. Vasconcelos and A. Cavaco-Paulo, *Cellulose*, 2006, **13**, 611.
- 12 M. Wada, Y. Nishiyama, H. Chanzy, T. Forsyth and P. Langan, *Powder Diffr.*, 2008, **23**, 92.
- 13 M. Samir, F. Alloin and A. Dufresne, *Biomacromolecules*, 2005, **6**, 612.
- 14 M. J. John and S. Thomas, *Carbohydr. Polym.*, 2008, **71**, 343.
- 15 J. Pan, *Biochem. Eng. J.*, 2007, **35**, 183.
- 16 M. Amiri, S. Shahrokhian and F. Marken, *Electroanalysis (N. Y.)*, 2007, **19**, 1032.
- 17 M. Javanbakht, M. R. Ganjali, P. Norouzi, M. Abdouss and S. Riahi, *Anal. Lett.*, 2008, **41**, 619.
- 18 N. Gajovic, G. Binyamin, A. Warsinke, F. W. Scheller and A. Heller, *Anal. Chem.*, 2000, **72**, 2963.
- 19 M. J. Bonne, E. V. Milsom, M. Helton, W. Thielemans, S. Wilkins and F. Marken, *Electrochem. Commun.*, 2007, **9**, 1985.
- 20 (a) M. J. Bonne, K. J. Edler, J. G. Buchanan, D. Wolverson, E. Psillakis, M. Helton, W. Thielemans and F. Marken, *J. Phys. Chem. C*, 2008, **112**, 2660; (b) W. Thielemans, C. R. Warbey and D. A. Walsh, *Green Chem.*, 2009, **11**, 531.
- 21 K. Tsourounaki, M. J. Bonné, W. Thielemans, E. Psillakis, M. Helton, A. McKee and F. Marken, *Electroanalysis (N. Y.)*, 2008, **20**, 2395.
- 22 J. P. Lorand and J. O. Edwards, *J. Org. Chem.*, 1959, **24**, 769.
- 23 T. D. James, K. Sandanayake and S. Shinkai, *Angew. Chem., Int. Ed. Engl.*, 1996, **35**, 1911.
- 24 L. I. Bosch, T. M. Fyles and T. D. James, *Tetrahedron*, 2004, **60**, 11175.
- 25 S. Takahashi, S. Kurosawa and J. I. Anzai, *Electroanalysis (N. Y.)*, 2008, **20**, 816.
- 26 E. Granot, R. Tel-Vered, O. Lioubashevski and I. Willner, *Adv. Funct. Mater.*, 2008, **18**, 478.
- 27 *Boronic Acids in Organic Synthesis and Chemical Biology*, ed. D. G. Hall, Wiley-VCH, Weinheim, 2005, p. 61.
- 28 T. D. James, M. D. Phillips and S. Shinkai, *Boronic Acids in Saccharide Recognition*, The Royal Society of Chemistry, Cambridge, 2006.
- 29 R. Tuytten, F. Lemiere, W. Van Dongen, E. Witters, E. L. Esmans, R. P. Newton and E. Dudley, *Anal. Chem.*, 2008, **80**, 1263.
- 30 S. Senel, *Colloids Surf., A: Physicochemical and Engineering Aspects*, 2003, **219**, 17.
- 31 W. J. Lyons, *J. Chem. Phys.*, 1941, **9**, 377.
- 32 P. Terech, L. Chazeau and J. Y. Cavaille, *Macromolecules*, 1999, **32**, 1872.
- 33 Y. Nishiyama, J. Sugiyama, H. Chanzy and P. Langan, *J. Am. Chem. Soc.*, 2003, **125**, 14300.
- 34 A. Isogai, M. Usuda, T. Kato, T. Uryu and R. H. Atalla, *Macromolecules*, 1989, **22**, 3168.
- 35 M. Wada, Y. Nishiyama, H. Chanzy, T. Forsyth and P. Langan, *Powder Diffr.*, 2008, **23**, 92.
- 36 Y. Kubo, T. Ishida, A. Kobayashi and T. D. James, *J. Mater. Chem.*, 2005, **15**, 2889.
- 37 W. Sun and K. Jiao, *Talanta*, 2002, **56**, 1073.
- 38 S. Arimori, C. J. Ward and T. D. James, *Tetrahedron Lett.*, 2002, **43**, 303.
- 39 V. E. Mouchrek, A. L. B. Marques, J. J. Zhang and G. O. Chierice, *Electroanalysis (N. Y.)*, 1999, **11**, 1130.
- 40 J. Yan, G. Springsteen, S. Deeter and B. Wang, *Tetrahedron*, 2004, **60**, 11205.
- 41 S. Murcia-Mascaros, C. Domingo, S. Sanchez-Cortes, M. V. Canameres and J. V. Garcia-Ramos, *J. Raman Spectrosc.*, 2005, **36**, 420.
- 42 G. Springsteen and B. H. Wang, *Tetrahedron*, 2002, **58**, 5291.
- 43 S. Arimori, C. J. Ward and T. D. James, *Tetrahedron Lett.*, 2002, **43**, 303.
- 44 V. Mirceski and M. Lovric, *Electroanalysis (N. Y.)*, 1997, **9**, 1283.